Relationship between intracranial pressure and phase-contrast cine MRI-derived measures of cerebrospinal fluid parameters in communicating hydrocephalus

Jia Long[1#], Hai Lin[2#], Gan Cao[3], Meng-Zhu Wang[4], Xian-Jian Huang[2], Jun Xia[1], Zhonghua Sun[5]

[1]Department of Radiology, [2]Department of Neurosurgery, The First Affiliated Hospital of Shenzhen University/Shenzhen Second People's Hospital, Shenzhen University Health Science Center, Shenzhen 518035, China; [3]Department of Radiology, Shenzhen Second People's Hospital, Clinical Medicine College of Anhui Medical University, Shenzhen 518000, China; [4]MR Scientific Marketing, Siemens Healthineers, Guangzhou 510145, China; [5]Discipline of Medical Radiation Sciences, School of Molecular and Life Sciences, Curtin University, Perth, WA, Australia

[#]These authors contributed equally to this work.

Correspondence to: Jun Xia, MD, PhD. Department of Radiology, The First Affiliated Hospital of Shenzhen University, Health Science Center, Shenzhen Second People's Hospital, Shenzhen 518035, China. Email: xiajun@email.szu.edu.cn; Zhonghua Sun, MD, PhD. Discipline of Medical Radiation Sciences, School of Molecular and Life Sciences, Curtin University, GPO Box U1987, Perth, WA 6845, Australia. Email: z.sun@curtin.edu.au.

Background: To explore the correlation between intracranial pressure (ICP) and cerebrospinal fluid (CSF) parameters assessed by phase-contrast cine MRI (PC-MRI).

Methods: Fifteen normal people and 80 subjects with communicating hydrocephalus who underwent PC-MRI examinations from a single center were included in this cross-sectional study. In addition to recording patient's age, heart rate, blood pressure and body mass index (BMI), ICP and CSF hemodynamic parameters, such as flow velocity and aqueduct diameter, were measured for correlation analysis.

Results: The mean ICP and CSF aqueduct diameter in hydrocephalus patients were 151.05 mmH$_2$O and 2.877 mm, respectively, and the maximum (6.938 cm/s) and mean (0.845 cm/s) CSF flow velocities were significantly higher in these patients compared with the controls (P<0.05). After adjusting for age, heart rate, blood pressure, and BMI, there was no significant relationship between peak velocity and ICP (P>0.05). Furthermore, a nonlinear relationship was observed between the ICP and the average velocity of CSF, and the ICP and aqueduct diameter. The ICP increased with the average velocity above 1.628 cm/s (P≤0.01), and the aqueduct diameter increased more than 3.6 mm (P<0.001).

Conclusions: This study found significant correlations between ICP and average velocity and aqueduct diameter. These findings can be useful in assisting clinicians in predicting ICP more effectively, thus improving patient management.

Keywords: Intracranial pressure (ICP); phase-contrast cine MRI (PC-MRI); cerebrospinal fluid (CSF); correlation; parameters

Introduction

Hydrocephalus is a buildup of fluid in the ventricles of the brain, which can be caused by a range of different factors (1). In adults, acquired hydrocephalus is more prevalent and is mainly caused by subarachnoid hemorrhage, intracranial inflammation, brain tumors, brain trauma, and surgical complications (2-6). The typical manifestation of hydrocephalus is a clinically significant increase in

1414

Long et al. PC-MRI measurements in communicating hydrocephalus

intracranial pressure (ICP), defined as an increase greater than 200 mmH$_2$O for at least 5 min (7). Elevated ICP can have devastating consequences if diagnosis and treatment are delayed (8). The onset of elevated ICP may be quite rapid as with traumatic brain injury (TBI) or epidural hematoma. A more difficult diagnostic situation transpires when elevated ICP occurs insidiously over a long interval of time.

Currently, the standard methods used for monitoring ICP are invasive examinations (9,10), mainly by external ventricular drain (EVD) or lumbar puncture. These methods have been associated with high rates of infection (up to 27%) (11-13), malposition (8.8%) (14), and hemorrhage (up to 18%) (14,15).

Phase-contrast cine MRI (PC-MRI) is a technology that can be used to noninvasively acquire information on fluid dynamics via computer software processing (16-20). PC-MRI is widely used in clinical practice to characterize the type of hydrocephalus, perform preoperative evaluations, select surgical methods, and provide prognostic hydrodynamic information (19-23). This method has high clinical value as it allows for the quantitative assessment of cerebrospinal fluid (CSF) dynamics parameters, which are essential for obtaining a timely and accurate diagnosis of hydrocephalus (19,20,23).

Although quantitative assessments of hydrodynamic parameters, such as flow velocity, have been conducted at the aqueductal level in patients with normal pressure hydrocephalus (19,20,23), little is known about the relationship among ICP and CSF parameters that are determined noninvasively based on PC-MRI. The purpose of this study was to explore the correlations between these hydrodynamic parameters measured using PC-MRI and changes in ICP in patients with communicating hydrocephalus.

Methods

Patients and management

This study consisted of normal participants and patients with communicating hydrocephalus who were recruited from November 2017 to August 2018 at our clinical practice. Normal participants only underwent MRI examination, while the patients with hydrocephalus received both MRI and lumbar puncture examinations. Age, gender, heart rate, blood pressure, body weight, and height (to calculate body mass index-BMI) were recorded. As part of the routine

diagnostic management for hydrocephalus, all patients had phase-contrast cine MRI CSF flow studies, followed by a continuous lumbar puncture on the same day. Patients had standard axial T2WI to calculate Evan's index and measure the aqueduct diameter by three-dimensional reconstructions. The Evan's index is defined as the ratio of the maximum distance between the anterior horns of the lateral ventricles on both sides and the maximum diameter of the cranial cavity on the same level (22); an index of ≥0.3 indicates pathologic ventricular enlargement. The study was approved by our hospital Human Research Ethics Committee and was performed in accordance with the relevant provisions of the Helsinki Declaration on the ethics of clinical research. Informed consent was obtained from all patients.

Inclusion criteria were as follows: (I) patients with clinically suspected or diagnosed communication hydrocephalus; (II) MRI showing ventricular enlargement, Evan's index greater than 0.3, but with normal sulcus. Exclusion criteria were as follows: (I) patients with complete obstructive hydrocephalus; (II) Patients unsuited or unwilling to do a lumbar puncture and MRI; (III) suboptimal image quality for assessment and clinical diagnosis.

CSF pressure measurements

CSF pressure was measured by an experienced senior neurosurgeon with 10 years of experience in neurosurgery. The patient was instructed to lay in the lateral position, and the intervertebral space was punctured from the lumbar vertebra 2 to sacrum 1 (mainly at the lumbar 3–4 vertebrae) following a routine procedure for lumbar puncture (24). Blood pressure was measured in the supine position just before lumbar puncture was performed.

MRI sequences

All MRI images were obtained using a 3.0T MRI scanner (Prisma, Siemens, Erlangen, Germany) with 20-channel phase-array head coils. All patients underwent conventional MRI scanning, including axial T2WI and a retrospective cardiac-gated phase-contrast flow quantification sequence. The acquisition parameters for axial T2WI were as follows: TR/TE, 4,000/117 ms; the field of view, 220×220 mm; slice thickness/slice intervals, 6/1.8 mm; acquisition time, 96 s; flip angle, 90°. The acquisition parameters for PC-MRI were as follows: TR/TE, 21/7 ms; the field of view, 160× 160 mm; slice thickness/slice intervals, 6/1.2 mm; velocity encoding, 15 cm/s; acquisition time, ~183 s; flip angle, 10°.
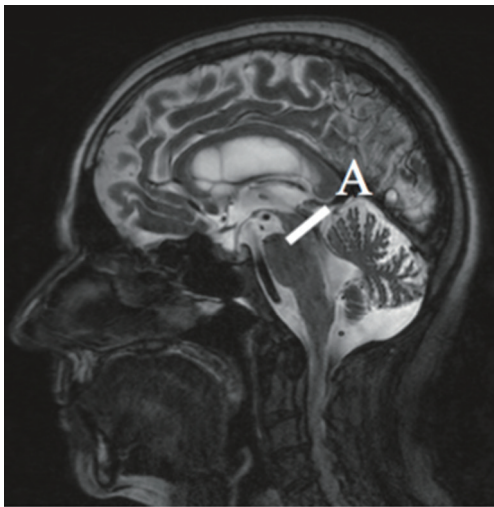
Figure 1 Midsagittal T_2 MRI depicting cerebral aqueduct. The image shows the position of the oblique slices for the cerebral aqueduct (A).

Image analysis

Image processing of the MRI data was performed independently by two radiologists who had 8 and 10 years of experience in brain MRI interpretation. The plane of selection was chosen to pass through the mid-portion of the aqueduct perpendicular to the direction of CSF flow to measure the aqueduct diameter (*Figure 1*). Regions of interest in the aqueduct were defined using axial phase images, and the subsequent quantitative analysis of CSF flow was performed using the Flow Quantification analysis software (Siemens, Erlangen, Germany) provided with the magnetic resonance scanner.

Statistical analysis

All analyses were performed using EmpowerStats (http://www.empowerstats.com) and the statistical package R (version 3.2.3). Descriptive statistics are expressed as the mean ± SD and were used to summarize baseline characteristics. The t-test method was used to verify whether the CSF dynamic parameters between the healthy control group and the hydrocephalus group were significantly different. In the hydrocephalus group, peak velocities, average velocities of CSF flow, and aqueduct diameter were each divided into tertiles (T1–3) to create a new categorical variable, and trend tests were performed by modeling the tertile (T1–3) peak velocities and average

velocities as continuous variables. We further applied a two-piecewise linear regression model to examine the threshold effect of the corrections between ICP and the peak CSF velocity, average CSF velocity, and aqueduct diameter using a smoothing function. The threshold level was determined using trial and error, including the selection of turning points along with a pre-defined interval and then choosing the turning point that provided the maximum model likelihood. We also conducted a log likelihood ratio test comparing the one-line linear regression model with a two-piecewise linear model. A two-sided P value <0.05 was considered to be statistically significant.

Results

A total of 122 participants were screened for communicating hydrocephalus, and 80 eligible patients were ultimately recruited. Five patients were excluded because they were unable to undergo an MRI scan or did not cooperate during the scan, 31 patients with complete obstructive hydrocephalus were excluded, and 6 patients were further excluded because they were unwilling to do a lumbar puncture or their ICP measurement was otherwise unobtainable. Eighty patients (45 men and 35 women; mean age, 57; age range, 22–78 years old) were included in the final analysis (*Figure 2*). The baseline demographic characteristics of the study population are summarized in *Table 1*. Fifteen normal participants were included as healthy controls, and CSF dynamic parameters were statistically different between the hydrocephalus group and healthy controls (*Table 2*).

Multiple linear regression models showed that baseline average CSF flow velocities (T1, T2) were positively associated with ICP after adjusting for sex, age, heart rate, baseline systolic blood pressure (SBP), baseline diastolic blood pressure (DBP), and BMI. However, baseline average velocity (T3) was inversely associated with ICP after adjustment for the abovementioned confounding factors.

The linear relationship between baseline average velocity and ICP was not statistically significant, suggesting that a nonlinear relationship might apply. Smoothing function also showed that ICP increased as peak velocity increased only within a certain range. Due to the nonlinear nature of this relationship, we further conducted a two-piecewise regression model analysis. We identified the turning point in baseline average velocity as 1.628 cm/s, corresponding to a predicted ICP value of 128.611 mmH$_2$O.
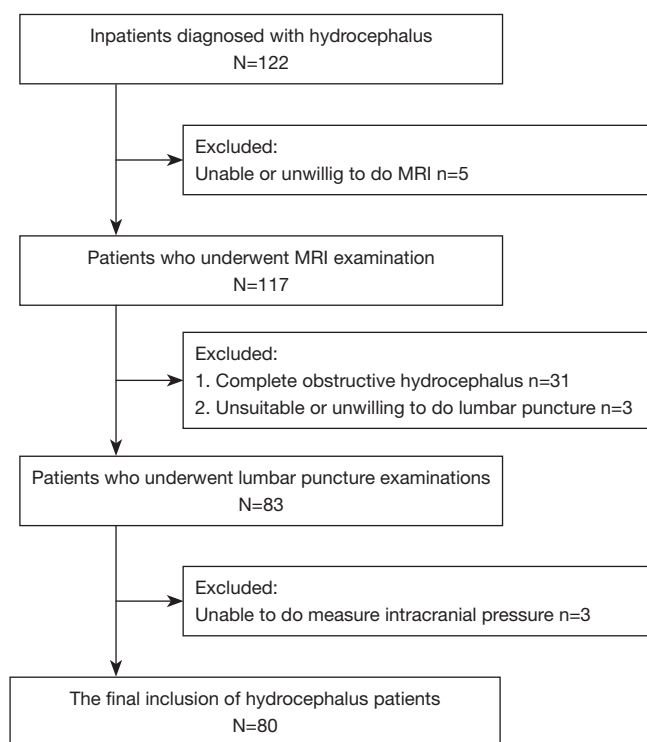
1416

Long et al. PC-MRI measurements in communicating hydrocephalus

Figure 2 Flowchart of hydrocephalus participant enrollment. MRI, magnetic resonance imaging.

Table 1 Baseline characteristics of study participants

Characteristics	Hydrocephalus group (n=80)	Healthy control (n=15)
Age (Y)	57.763±14.739	56.356±15.076
Heart rate (BPM)	81.737±14.193	81.156±14.994
SBP (mmHg)	131.037±20.469	123.178±20.842
DBP (mmHg)	80.850±10.243	78.089±10.293
BMI	23.195±1.846	23.648±1.543
Evan's index	0.403±0.059	–

BPM, beats per minute; SBP, systolic blood pressure; DBP, diastolic blood pressure; BMI, body mass index.

Hence, when the average CSF flow velocity was less than 1.628 cm/s, ICP decreased by 25.274 mmH$_2$O for each increase of one unit in average velocity (P>0.05). When the average velocity was greater than 1.628 cm/s, ICP increased by 63.208 mmH$_2$O for each increase in one unit in average velocity (P≤0.01). However, the correlation between ICP and peak CSF flow velocity was not significant.

Table 2 CSF flow dynamics of hydrocephalus and control subjects

Hemodynamic parameters	Hydrocephalus control (n=80)	Healthy control (n=15)	P value
Peak velocity (cm/s)	6.938±4.982	4.264±1.091	<0.05
Average velocity (cm/s)	0.845±0.824	0.426±0.630	<0.05
Aqueduct diameter (mm)	2.877±0.876	2.103±0.230	<0.05

CSF, cerebrospinal fluid.

Furthermore, we found a nonlinear relationship between ICP and aqueduct diameter. The turning point in aqueduct diameter was 3.6 mm, and the predicted ICP value at the turning point was 145.447 mmH$_2$O. When the aqueduct diameter was less than 3.6 mm, ICP increased by 9.836 mmH$_2$O for each increase of one unit in aqueduct diameter (P>0.05). When the aqueduct diameter was greater than 3.6 mm, ICP increased by 75.976 mmH$_2$O for each increase of one unit in aqueduct diameter (P<0.001). These results are presented in *Table 3* and *Figure 3*.

The intraclass correlation coefficients for interobserver and intraobserver agreement assessment was excellent about peak CSF velocity (0.937, 0.959), average CSF velocity (0.901, 0.926) and aqueduct diameter (0.859, 0.874), respectively. This suggests a robust reproducibility of PC-MRI.

Discussion

This study investigated the relationship between ICP and PC-MRI-derived CSF flow dynamic parameters in patients with communicating hydrocephalus. Our results show that when the average CSF flow velocity was greater than 1.628 cm/s and the aqueduct diameter was greater than 3.6 mm, ICP significantly increased. This indicates that the approximate value of ICP can be estimated by PC-MRI technique, which provides a new technical approach for rapid identification of intracranial hypertension in early clinical stage.

Previous studies reported that there was no significant correlation between ICP and peak CSF flow velocity, which is consistent with our results (25,26). Our study, however, did find a direct relationship between ICP and average CSF flow velocity. Previous studies may not reveal any significant correlations between CSF flow velocity and ICP because they considered only a potential linear relationship between these two variables, rather than a nonlinear relationship.

Table 3 The non-linear relationship between aqueduct diameter and ICP, and average velocity and ICP

Hemodynamic parameters	Turning point (K)	Adjusted ß/OR (95% CI)	P value
Aqueduct diameter (mm)	<3.6	9.836 (−8.979, 28.651)	0.309
	≥3.6	75.976 (42.013, 109.939)	<0.001
	ICP in turning point	145.447 (124.921, 165.974)	–
Average velocity (cm/s)	<1.628	−25.274 (−50.406, −0.142)	0.052
	≥1.628	63.208 (15.837, 110.579)	≤0.01
	ICP in turning point	128.611 (100.440, 156.783)	–

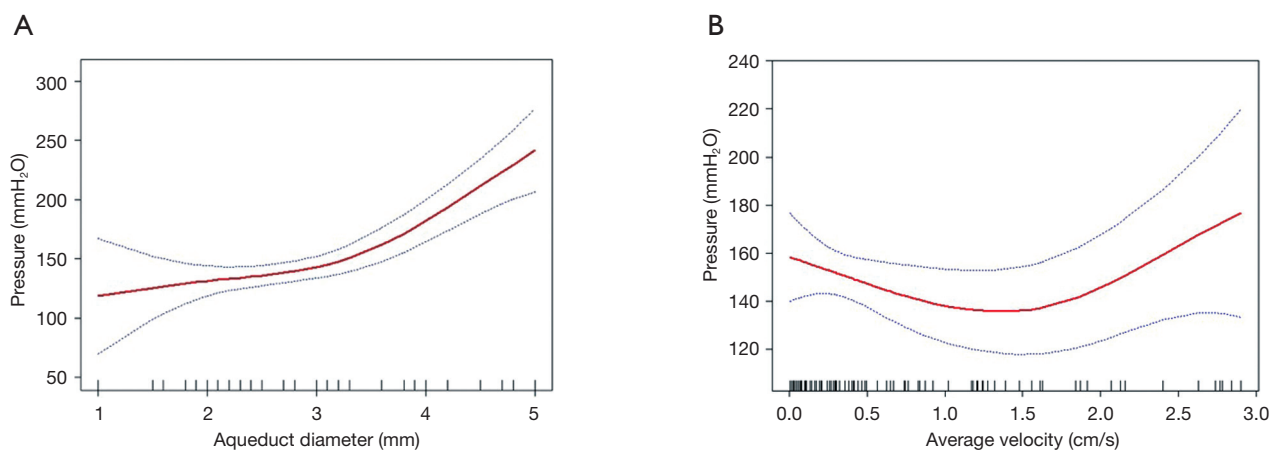ICP, intracranial pressure.

Figure 3 A cubic spline smoothing of intracranial pressure and aqueduct diameter (A), and of intracranial pressure and average velocity of cerebrospinal fluid (B).

Also, the CSF dynamics data used in their studies were obtained using images generated by two MRI machines with different Tesla values (1.5T and 3.0T). The different field strengths may have affected their results, due to the reduced noise level; flow measurements at 3T tolerate a larger deviation from the ideal encoding velocity than a 1.5T scanner, especially when applied to slow-flow velocities (27).

Xie *et al.* reported that when lumbar CSF pressure was within a certain range, ICP determined by lumbar puncture was significantly correlated with the width of the orbital space, as determined by MRI (28). The subarachnoid space around the optic nerve is continuous through the optic canal and the subarachnoid space. The study by Xie *et al.* thus predicts that changes in ICP are correlated with changes in the width of the subarachnoid space around the eyelid. Similarly, our findings suggest that changes in the width of the midbrain aqueduct can predict changes in ICP. PC-MRI can quantitatively assess CSF hydrodynamic

changes at the aqueductal level in relation to ICP values (19,20,23-25). However, to the best of our knowledge, no previous studies have reported a correlation between cerebral aqueduct diameters and ICP changes as evaluated by PC-MRI. Therefore, the findings of this study add valuable information to the current literature. Xie's study did not consider the effect of age on results. It has been reported that age is an important factor that affects ICP, and indeed, ICP seems to decrease with age by linear regression (29). Thus, we evaluated age as an adjusted variable, after controlling the effect of age, our results may be closer to the real situation.

Our findings have clinical value in two main areas: first, the relationships that we noninvasively identified between ICP and CSF flow velocity and aqueduct diameter may be valuable for the evaluation of preoperative ICP in patients with hydrocephalus. This method might be applied to identify whether ICP is increased quickly. Although MRI

scanning is a relatively long process, in our study, the acquisition time of the axial T2 and PC-MRI scans was about 5 min, and the duration of the image processing was about 3 min, which overall is less than 10 min in total and is suitable for imaging outpatients and inpatients. The subjects for lumbar puncture examination must be hospitalized for observation. After a series of lumbar puncture operations, the patients need to rest in bed for 4–6 h. In brief, non-invasive MRI examination provides clinicians with effective ICP measurements and more comprehensive image information, and thus, it can be used as a reliable and efficient technique for routine diagnosis.

Second, the current treatment for communicating hydrocephalus is ventricle-peritoneal shunt. The shunt device is widely used as it has an adjustable pressure valve that can adjust the shunt speed *in vitro* to reduce the occurrence of postoperative complications. However, there is little consensus as to how to set the pressure to achieve the best situation. Adjusting the valve speed based on the improvement of the patient's clinical symptoms and the clinician's experience is a highly subjective process. Furthermore, the invasiveness of lumbar puncture may cause harm to the postoperative patient (30). Therefore, postoperative evaluation can be carried out by MRI, and ICP can, in turn, be measured based on the direct relationship between ICP and CSF flow velocity and aqueduct diameter. This may help in setting an optimal valve velocity value to adjust the shunt threshold and avoid potential secondary injury caused by lumbar puncture.

This study has some limitations. First, it is a cross-sectional study, and therefore, we only derived correlations between two variables and could not derive causal relationships. Second, since we only selected patients with communicating hydrocephalus, the results of this study do not apply to patients with complete obstructive hydrocephalus. This limitation could be resolved in future studies that include patients with different types of hydrocephalus. Third, since the PC-MRI and the lumbar puncture examination are not performed at the same time, the results may be affected to some extent, although we do not expect any significant impact on our findings. Simultaneous synchronized ICP recording and MRI could be another future research direction allowing for immediate correlation between ICP and these cerebral dynamic parameters.

In conclusion, we observed the relationships between ICP and cerebral hydrodynamic parameters assessed using noninvasive PC-MRI, and the significant non-linear relationships between ICP and aqueduct diameter, and

between ICP and average CSF flow velocity. These findings have potentially significant clinical value as they could guide clinicians to manage patients with hydrocephalus more effectively. Although we do not suggest that the PC-MRI replace invasive ICP monitoring, this technique might be helpful for patients who are ill-suited for invasive assessments.

Footnote

Conflicts of Interest: The authors have no conflicts of interest to declare.

Ethical Statement: The study was approved by the hospital Human Research Ethics Committee and was performed in accordance with the relevant provisions of the Helsinki Declaration on the ethics of clinical research. Informed consent was obtained from all patients.

References

1. Reith W, Yilmaz U. Hydrocephalus and intracranial hypotension. Radiologe 2012;52:821-6.
2. Murata T, Horiuchi T, Hongo K. Management of Hydrocephalus Following SAH and ICH. In: Ahmed Ammar. editors. Hydrocephalus. New York: Springer, 2017;191-200.
3. Jusue-Torres I, Lu J, Sankey EW, Vivas-Buitrago T, Crawford J, Pletnikov M, Xu J, Blitz A, Crain B, Hulbert A, Guerrero-Cazares H, Gonzalez-Perez O, Quiñones-Hinojosa A, McAllister P, Rigamonti D. Association between inflammatory extension and the ventricular size in adult chronic communicating hydrocephalus: An experimental model of adult hydrocephalus. Fluids Barriers CNS 2015;12:O57.
4. Cipri S, Gangemi A, Cafarelli F, Messina G, Iacopino P, Al Sayyad S, Capua A, Comi M, Musitano A. Neuroendoscopic management of hydrocephalus

secondary to midline and pineal lesions. J Neurosurg Sci 2005;49:97-106.

5. Yoon JE, Lee CY, Sin EG, Song J, Kim HW. Clinical Feature and Outcomes of Secondary Hydrocephalus Caused by Head Trauma. Korean J Neurotrauma 2018;14:86-92.

6. Takai K, Komori T, Shin M, Niimura M, Taniguchi M. Superficial siderosis complicated by hydrocephalus:bleeding from the dura mater in the cerebrospinal fluid cavity after brain tumor surgery. Acta Neurochirurgica 2016;158:1299-302.

7. Downard C, Hulka F, Mullins RJ, Piatt J, Chesnut R, Quint P, Mann NC. Relationship of Cerebral Perfusion Pressure and Survival in Pediatric Brain-Injured Patients. J Trauma 2000;49:654-8.

8. Czosnyka M. Monitoring and interpretation of intracranial pressure. J Neurol Neurosurg Psychiatry 2004;75:813-21.

9. Smith M. Monitoring Intracranial Pressure in Traumatic Brain Injury. Anesth Analg 2008;106:240-8.

10. Speck V, Staykov D, Huttner HB, Sauer R, Schwab S, Bardutzky J. Lumbar Catheter for Monitoring of Intracranial Pressure in Patients with Post-Hemorrhagic Communicating Hydrocephalus. Neurocrit Care 2011;14:208-15.

11. Koskinen LO, Grayson D, Olivecrona M. The complications and the position of the Codman MicroSensorTM ICP de- vice:an analysis of 549 patients and 650 sensors. Acta Neurochir 2013;155:2141-8.

12. Hoefnagel D, Dammers R, Ter Laak-Poort MP, Avezaat CJ. Risk factors for infections related to external ventricular drainage. Acta Neurochir 2008;150:209-14.

13. Karvellas CJ, Fix OK, Battenhouse H, Durkalski V, Sanders C, Lee WM; U S Acute Liver Failure Study Group. US Acute Liver Failure Study Group. Outcomes and Complications of Intracranial Pressure Monitoring in Acute Liver Failure: A Retrospective Cohort Study. Crit Care Med 2014;42:1157-67.

14. Anderson RC, Kan P, Klimo P, Brockmeyer DL, Walker ML, Kestle JR. Complications of intracranial pressure monitoring in children with head trauma. J Neurosurg 2004;101:53-8.

15. Binz DD, Toussaint LG, Friedman JA. Hemorrhagic complications of ventriculostomy placement: a meta-analysis. Neurocrit Care 2009;10:253-6.

16. Pelc NJ, Herfkens RJ, Shimakawa A, Enzmann DR. Phase contrast cine magnetic resonance imaging, Magn Reson Q 1991;7:229-254.

17. Powell AJ, Maier SE, Chung T, Geva T. Phase-Velocity Cine Magnetic Resonance Imaging Measurement of Pulsatile Blood Flow in Children and Young Adults: In Vitro and In Vivo Validation. Pediatr Cardiol 2000;21:104-10.

18. Enzmann DR, Pelc NJ. Normal flow patterns of intracranial and spinal cerebrospinal fluid defined with phase-contrast cine MR imaging. Radiology 1991;178:467-74.

19. Lindstrøm EK, Ringstad G, Mardal KA, , Eide PK. Cerebrospinal fluid volumetric net flow rate and direction in idiopathic normal pressure hydrocephalus. Neuroimage Clin 2018;20:731-41.

20. Gokul UR, Ramakrishnan KG. Change in average peak cerebrospinal fluid velocity at the cerebral aqueduct, before and after lumbar CSF tapping by the use of phase contrast MRI, and its effect on gait improvement in patients with normal pressure hydrocephalus. Neurol India 2018;66:1407-12.

21. Miyamoto J, Tatsuzawa K, Sasajima H, Mineura K. Usefulness of phase contrast cine mode magnetic resonance imaging for surgical decision making in patients with hydrocephalus combined with achondroplasia. Case report. Neurol Med Chir (Tokyo) 2010;50:1116-8.

22. Miskin N, Patel H, Franceschi AM, Ades-Aron B, Le A, Damadian BE, Stanton C, Serulle Y, Golomb J, Gonen O, Rusinek H, George AE; Alzheimer's Disease Neuroimaging Initiative. Diagnosis of Normal-Pressure Hydrocephalus Use of Traditional Measures in the Era of Volumetric MR Imaging. Radiology 2017;285:197-205.

23. Ringstad G, Emblem KE, Eide PK. Phase-contrast magnetic resonance imaging reveals net retrograde aqueductal flow in idiopathic normal pressure hydrocephalus. J Neurosurg 2016;124:1850-7.

24. Wright BL, Lai JT, Sinclair AJ. Cerebrospinal fluid and lumbar puncture: a practical review. J Neurol 2012;259:1530-45.

25. Jaeger M, Khoo AK, Conforti DA, Cuganesan R. Relationship between intracranial pressure and phase contrast cine MRI derived measures of intracranial pulsations in idiopathic normal pressure hydrocephalus. J Clin Neurosci 2016;33:169-72.

26. Hamilton R, Baldwin K, Fuller J, Vespa P, Hu X, Bergsneider M. Intracranial pressure pulse waveform correlates with aqueductal cerebrospinal fluid stroke volume. J Appl Physiol 2012;113:1560-6.

27. Lotz J, Döker R, Noeske R, Schüttert M, Felix R, Galanski M, Gutberlet M, Meyer GP. In vitro validation of phase-contrast flow measurements at 3T in comparison to 1.5 T: Precision, accuracy, and signal-to-noise ratios. J Magn Reson Imaging 2005;21:604-10.

1420

Long et al. PC-MRI measurements in communicating hydrocephalus

28. Xie X, Zhang X, Fu J, Wang H, Jonas JB, Peng X, Tian G, Xian J, Ritch R, Li L, Kang Z, Zhang S, Yang D, Wang N; Beijing iCOP Study Group. Noninvasive intracranial pressure estimation by orbital subarachnoid space measurement: the Beijing Intracranial and Intraocular Pressure (iCOP) study. Crit Care 2013;17:R162.

29. Pedersen SH, Lilja-Cyron A, Andresen M, Juhler M. The Relationship Between Intracranial Pressure and Age—

Chasing Age-Related Reference Values. World Neurosurg 2018;110:e119-23.

30. Eide PK, Sorteberg W. Changes in intracranial pulse pressure amplitudes after shunt implantation and adjustment of shunt valve opening pressure in normal pressure hydrocephalus. Acta Neurochirurgica 2008;150:1141-7.